

Magnetic Properties of Exchange-Biased $[\text{Co}/\text{Pt}]_n$ Multilayer With Perpendicular Magnetic Anisotropy

Jun-Yang Chen^{1,2}, Jia-Feng Feng¹, Zhu Diao¹, Gen Feng¹, J. M. D. Coey¹, and Xiu-Feng Han²

¹CRANN and School of Physics, Trinity College, Dublin 2, Ireland

²Beijing National Lab of Condensed Matter Physics, Institute of Physics, Chinese Academy of Sciences, Beijing 100190, China

Perpendicular exchange-biased $[\text{Co}/\text{Pt}]_3/\text{Co}(t_{\text{Co}})/\text{IrMn}$ and $\text{IrMn}/\text{Co}(t_{\text{Co}})/\text{Pt}/[\text{Co}/\text{Pt}]_3$ multilayers have been fabricated, changing the thickness (t_{Co}) of the cobalt that is next to the IrMn layer. The crystal structure, interface roughness and magnetic properties were characterized by X-ray diffraction (XRD), X-ray reflectivity (XRR), atomic force microscopy (AFM) and extraordinary Hall Effect (EHE). The multilayers are flat, and the roughness is about 0.2 nm across the 2- μm scanning range. The magnetization reversal is dependent on t_{Co} , and the exchange bias and coercivity vary with t_{Co} . The exchange bias reaches a maximum value (about 13.9 mT) for top-pinned multilayers at $t_{\text{Co}} = 0.45$ nm, while it reaches a maximum (about 3.5 mT) for bottom-pinned multilayers at $t_{\text{Co}} = 0.6$ nm. For both stacks the coercivity is maximum (about 30 mT) at $t_{\text{Co}} = 0.8$ nm, and stable for $t_{\text{Co}} > 1.0$ nm. These results are well understood in terms of the Co spin orientation at the Co/IrMn interface.

Index Terms— $[\text{Co}/\text{Pt}]_n$ perpendicular multilayers, magnetization reversal.

I. INTRODUCTION

THE phenomenon of exchange bias (EB) between ferromagnetic (FM) and antiferromagnetic (AFM) films, leading to a shift in the hysteresis loop of the ferromagnet, has attracted much attention because of the rich and controversial physics, and the potential applications of exchange bias in magnetic memory and sensors based on spin valves or magnetic tunnel junctions (MTJ) [1]–[5]. Usually, the phenomenon is studied in FM-AFM bilayers with in-plane anisotropy. More recently, perpendicular exchange bias has been investigated in continuous or nano-structured magnetic perpendicular multilayers [6]–[13]. Among these systems, $[\text{Co}/\text{Pt}]_n$ or $[\text{Co}/\text{Pd}]_n$ multilayers are often used, and they are coupled with an AFM layer, such as CoO [6], [7], NiO [8], FeMn [9], [12] or IrMn [10], [11], [13]. There are several parameters that influence the perpendicular anisotropy, such as the period (n) of multilayers and the relative thickness of Co, Pt or Pd. It is found that increasing n increases the perpendicular exchange bias [14]. Exchange bias is essentially determined by the orientation of the local magnetic moment on the surface of the Co layer that couples with the AFM layer. For example, experiments on exchange-biased $[\text{Co}/\text{Pt}]_n$ multilayers have shown that the exchange bias was enhanced by inserting an ultrathin Pt layer at the Co/IrMn interface [10]–[13], which suggests that a thin Pt layer reorients the Co spin from a tilted orientation (due to the in-plane anisotropy at the Co/AFM interface) towards the normal to the AFM film. Until now, there have been few reports on the relation between the exchange bias and magnetization reversal in perpendicular $[\text{Co}/\text{Pt}]_n$ multilayers varying the orientation of the local moment of cobalt at Co/IrMn interface.

In this work, we have systematically investigated the top-pinned ($[\text{Pt}(2 \text{ nm})/\text{Co}(0.45 \text{ nm})]_3/\text{Pt}(2 \text{ nm})/\text{Co}(t_{\text{Co}})/$

$\text{IrMn}(10 \text{ nm})$) and bottom-pinned ($\text{IrMn}(10 \text{ nm})/\text{Co}(t_{\text{Co}})/[\text{Pt}(2 \text{ nm})/\text{Co}(0.45 \text{ nm})]_3$) perpendicular $[\text{Co}/\text{Pt}]_n$ multilayers by changing the thickness (t_{Co}) of the Co layer. The dependence of the exchange bias and the coercivity has been determined for varying t_{Co} , and a strong competition between the out-of-plane interfacial anisotropy and the in-plane anisotropy has been observed. There are significant differences between the top-pinned and bottom-pinned structures.

II. EXPERIMENTAL METHODS

Two series of $[\text{Co}/\text{Pt}]_n$ multilayers with complete layer sequences $[\text{Pt}(2)/\text{Co}(0.45)]_3/\text{Pt}(2)/\text{Co}(t_{\text{Co}})/\text{IrMn}(10)/\text{Pt}(2)$ and $\text{Pt}(2)/\text{IrMn}(10)/\text{Co}(t_{\text{Co}})/[\text{Pt}(2)/\text{Co}(0.45)]_3/\text{Pt}(2)$ were grown on thermally oxidized Si wafers; layer thicknesses are given in nanometers. All multilayers were grown under high vacuum at room temperature in a Shamrock sputtering tool [15]. The thickness (t_{Co}) of the Co layer that is next to the IrMn layer ranged from 0 to 5.0 nm. The out-of-plane magnetic hysteresis loops were measured using the extraordinary Hall Effect (EHE). For EHE measurements, square samples were contacted at the four corners in the Van der Pauw geometry. The thickness, the interface roughness and crystal structure were characterized by X-ray Reflectivity (XRR), Atomic Force Microscopy (AFM) and X-ray Diffraction (XRD), respectively.

III. RESULTS AND DISCUSSION

Fig. 1 shows typical X-ray reflectivity (XRR) spectra for top- and bottom-pinned $[\text{Co}/\text{Pt}]_n$ multilayers with $t_{\text{Co}} = 0.45$ nm. A good fitting is made after using the total thickness (21.8 nm) of the stacks. Furthermore, according to the equation below [16]

$$d = \lambda/2\Delta\theta \quad (1)$$

where d is the total thickness of sample, λ is the X-ray wavelength, $\Delta\theta$ is the oscillation period. The estimated thicknesses of bottom-pinned and top-pinned $[\text{Co}/\text{Pt}]_n$ multilayers are 21.1 nm and 21.3 nm, which is similar to what we intended (21.8 nm). Fig. 2 presents the XRD results for top- and bottom-pinned $[\text{Co}/\text{Pt}]_n$ multilayers. Two XRD peaks are attained (see the fitting lines), one belongs to (111)-oriented Pt, and the other is (111)-oriented IrMn, which shows the crystalline character of

Manuscript received October 27, 2009; revised December 27, 2009; accepted January 12, 2010. Current version published May 19, 2010. Corresponding authors: J. M. D. Coey and X.-F. Han (e-mail: jcoey@tcd.ie; xfhan@aphy.iphy.ac.cn).

Color versions of one or more of the figures in this paper are available online at <http://ieeexplore.ieee.org>.

Digital Object Identifier 10.1109/TMAG.2010.2041192

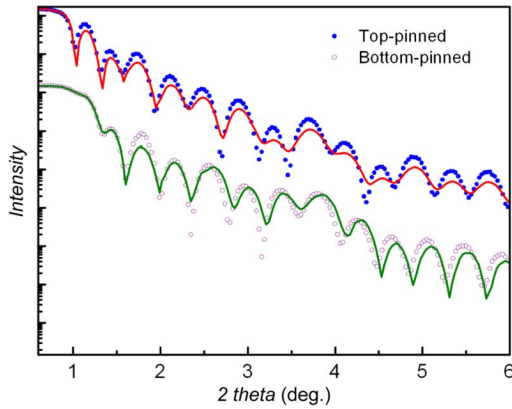


Fig. 1. Typical X-ray reflectivity (XRR) spectra of top- and bottom-pinned $[\text{Co}/\text{Pt}]_n$ multilayers with $t_{\text{Co}} = 0.45$ nm.

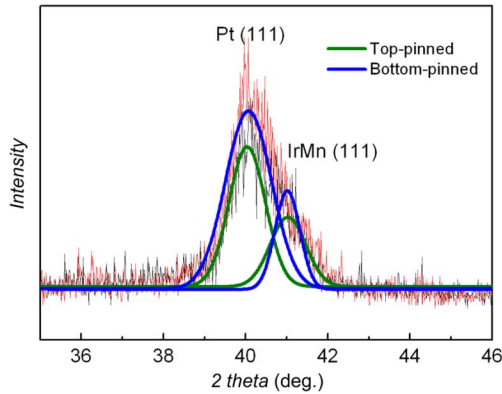


Fig. 2. High angular X-ray diffraction (XRD) of top- and bottom-pinned exchange-biased $[\text{Co}/\text{Pt}]_n$ multilayers, a broad peak about 40° is shown, which can be fitted by two peaks, one is Pt (111) and the other is IrMn (111).

these samples. A similar structural characterization is observed in [17]. The XRD peak is slightly higher for the bottom-pinned multilayers, and it may be due to a better crystalline structure.

Fig. 3 gives the out-of-plane EHE loops for top-pinned (a)–(h) and bottom-pinned (i)–(p) $[\text{Co}/\text{Pt}]_n$ multilayers by changing t_{Co} . Both $[\text{Co}/\text{Pt}]_n$ multilayers give a square hysteresis loop with almost 100% remnant magnetization. For top- and bottom-pinned samples, different sample shows different EHE loops. For example, as shown in Fig. 3(f) with $t_{\text{Co}} = 1.0$ nm, a little tilting is observed in the EHE loop when it goes to saturation. This is probably due to most of the moments of the Co layer has become aligned from out-of-plane to in-plane. As shown in Fig. 3(l) and Fig. 3(m) with $t_{\text{Co}} = 0.6$ and 0.8 nm, there exists a reversal asymmetry in the EHE loops. It is often attributed to the asymmetric nucleation process during the magnetization reversal [7], [18]. To understand the origin in these $[\text{Co}/\text{Pt}]_n$ stacks, the EHE loops of bottom-pinned $[\text{Co}/\text{Pt}]_n$ with $t_{\text{Co}} = 0.6$ nm are measured, as shown in Fig. 4, a little asymmetry is found in the 1st EHE loop, but the EHE loop becomes symmetry after measured 5 times. Here, the reversal asymmetry can be interpreted by the training effect, which is often observed in exchange biased systems [7], [19]–[21].

Fig. 5 summarizes the exchange bias and the coercivity as the function of t_{Co} . As shown in Fig. 5(a), the exchange bias increases first for both top- and bottom-pinned $[\text{Co}/\text{Pt}]_n$ multilayers. Then the exchange bias reaches a maximum (about 13.9

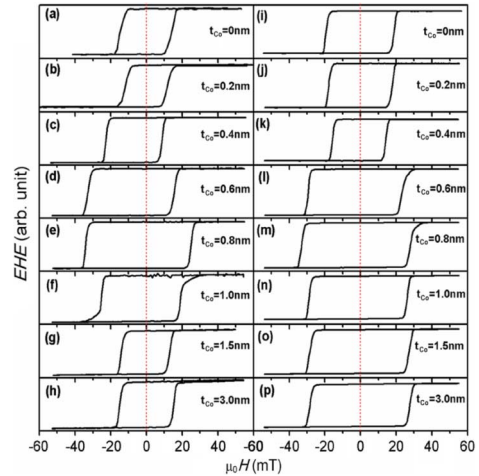


Fig. 3. Out-of-plane EHE hysteresis loops of top-pinned (a)–(h) and bottom-pinned (i)–(p) exchange-biased perpendicular $[\text{Co}/\text{Pt}]_n$ multilayers.

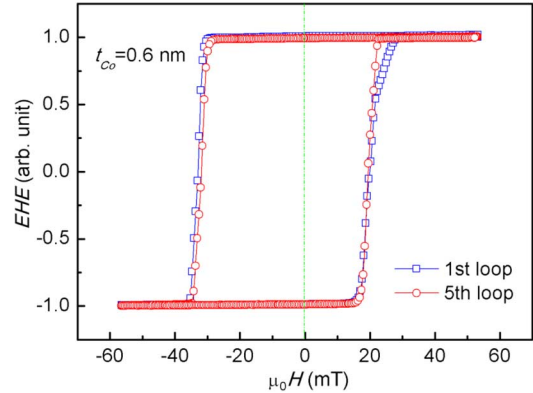


Fig. 4. Out-of-plane EHE hysteresis loops of bottom-pinned $[\text{Co}/\text{Pt}]_n$ multilayers with $t_{\text{Co}} = 0.6$ nm.

mT) for top-pinned samples at $t_{\text{Co}} = 0.45$ nm and it reaches the maximum (about 3.5 mT) for bottom-pinned samples at $t_{\text{Co}} = 0.6$ nm. After that, both decrease with increasing t_{Co} . The exchange bias is almost zero when t_{Co} is more than 1.5 nm for both configurations, which is similar to the results as reported in [11], [22]. The spin structure of the Co layer at the Co/IrMn interface is the key factor for perpendicular exchange bias. The perpendicular exchange bias is roughly proportional to the FM-AFM spin projection at the interface [11]. As shown in Meiklejohn and Bean's model, the exchange bias is written as [23], [24]

$$H_{eb} = \frac{JS_{AFM}S_{FM}}{\mu_0\alpha_{AFM}^2M_{FM}t_{FM}} \quad (2)$$

where J is the interface exchange energy, S_{AFM} and S_{FM} are the spin moments along the film normal in the AFM and FM interfacial layers, α_{AFM}^2 is the AFM unit cell size, M_{FM} is the magnetization of the FM layer and t_{FM} is the thickness of the FM layer. With the increase of t_{Co} , the Co layer shows very strong perpendicular anisotropy. The thin Co film exhibits an out-of-plane easy axis due to strong interfacial anisotropy for $t_{\text{Co}} < 1.0$ nm in $[\text{Co}/\text{Pt}]_n$ multilayers [6]. When the Co layer has $t_{\text{Co}} > 1.0$ nm, a competition between the out-of-plane interfacial anisotropy and the in-plane shape anisotropy shows in $[\text{Co}/\text{Pt}]_n$ multilayers. The effective anisotropy of the Co film

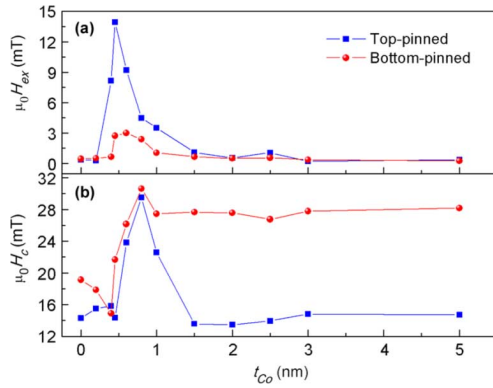


Fig. 5. Out-of-plane of exchange bias field (a) and coercivity (b) with the variety of Co thickness for top- and bottom- pinned of exchange-biased $[\text{Co}/\text{Pt}]_n$ multilayers.

gradually changes from out-of-plane perpendicular anisotropy to in-plane anisotropy.

A schematic structure of the top-pinned $[\text{Co}/\text{Pt}]_n$ stacks is shown in Fig. 6(a), and the domain structure of the Co layer for them with t_{Co} is given in Fig. 6(b)–(e). In these exchange-biased $[\text{Co}/\text{Pt}]_n$ stacks, when t_{Co} is 0.2 nm (a monolayer), the exchange bias is nearly zero due to the very thin Co layer, which is unlikely to form a continuous film, but some separated islands. For this case, the S_{FM} and S_{AFM} values are limited at the Co/IrMn interface. Furthermore, the separated islands may show superparamagnetism, as indicated in Fig. 6(b). With the increase of t_{Co} up to 0.4 nm, the exchange bias reaches about 8 mT. This suggests the interface area of Co/IrMn for the out-of-plane interfacial anisotropy becomes large. When t_{Co} is 0.45 nm, the highest exchange bias is obtained for top-pinned samples, which reflects the highest out-of-plane interfacial anisotropy. The Co layer may form a continuous film and a single domain state is formed, as shown in Fig. 6(c). Then, the exchange bias starts to decrease on increasing t_{Co} , which suggests the in-plane shape anisotropy has an influence on the exchange bias. Due to the competition between the in-plane shape anisotropy and out-of-plane interfacial anisotropy, multi-domain states occur and the effective Co spin may have a little tilting, which correspond to a decrease of the exchange bias with t_{Co} as shown in Fig. 5(a). With the further increase of t_{Co} (for instance, $t_{\text{Co}} = 1.5$ nm), the exchange bias is close to zero for both $[\text{Co}/\text{Pt}]_n$ stacks. The in-plane domain structure appears and there is no net perpendicular magnetic moment in the Co layer (Fig. 6(e)). From the above discussion, the magnetic structure of the Co layer may go from the random superparamagnetic, to out-of-plane single domain, out-of-plane multi-domain to the in-plane domain in the t_{Co} range of 0–5 nm [25]. However, there are other factors which may influence the exchange bias. For example, the layer roughness can increase pinning sites, and change the interfacial exchange coupling and AF uniaxial anisotropy, which also contributes to the exchange bias [26].

As for the coercive field, shown in Fig. 5(b) as a function of t_{Co} , it increases first, and reaches the maximum value (about 30 mT) at $t_{\text{Co}} = 0.8$ nm for both top- and bottom-pinned $[\text{Co}/\text{Pt}]_n$ multilayers. However, when t_{Co} is larger than 1.0 nm, coercivity is quite different for both configurations. For bottom-pinned $[\text{Co}/\text{Pt}]_n$ multilayers, the coercivity becomes stable after $t_{\text{Co}} > 1.0$ nm. But for top-pinned configurations,

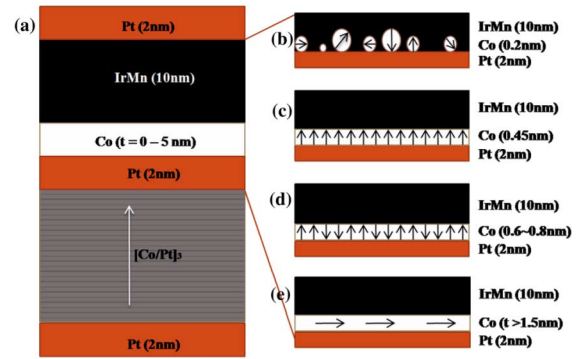


Fig. 6. A schematic structure of (a) typical top-pinned $[\text{Co}/\text{Pt}]_n$ multilayers. (b)–(e) the schematic domain structure of the Co layer with the increase of t_{Co} . The domain structure goes from random superparamagnetic (b), the out-of-plane single domain (c), the out-of-plane multi-domain (d) and in-plane domain (e).

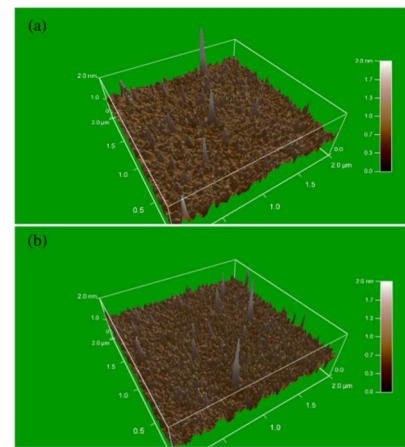


Fig. 7. AFM images for the surface roughness of (a) Pt/ $[\text{Co}/\text{Pt}]_3$ and (b) Pt/IrMn/Co(t_{Co})/Pt/ $[\text{Co}/\text{Pt}]_3$ multilayers with $t_{\text{Co}} = 2.0$ nm, which shows the roughness is 0.16 and 0.21 nm, respectively.

the coercivity does not become stable until $t_{\text{Co}} > 1.5$ nm and a much smaller value is observed.

To understand the coercivity change with the thickness of the Co layer, the spin model given by Mobley *et al.* [27] is used. According to this model, each spin is initially assigned an anisotropy field, defined as

$$H_k = 2K/(\mu_0 M_s) \quad (3)$$

where K is the anisotropy energy. $-H_k$ is the field at which an isolated spin would flip from up to down and conversely for $+H_k$. Thus each spin has its own reversal field and is inherently hysteretic. Comparing our data with this model, when t_{Co} increases from 0 to 0.8 nm, the total out-of-plane spin moment of the Co film monotonically increases. This explains the coercivity increase with the increase of t_{Co} for both $[\text{Co}/\text{Pt}]_n$ multilayers as shown in Fig. 5(b), which is consistent with (2). However, when t_{Co} is larger than 1.0 nm, the coercivity is quite different for both stacks. The net out-of-plane spin moment of Co is small, and the magnetization reversal mostly comes from the $[\text{Co}/\text{Pt}]_3$ multilayers. In this case, the roughness becomes dominant. Here XRD and AFM are measured, as shown in Fig. 2 and Fig. 7. XRD data show the crystal structure of the samples, and the AFM reflects the $[\text{Co}/\text{Pt}]_3$ interface roughness. For top- and bottom- pinned $[\text{Co}/\text{Pt}]_n$ multilayers, the roughness is 0.16 nm and 0.21 nm, respectively. To increase the layer thickness

will increase the roughness, and larger roughness comes from thicker bottom IrMn/Co layers. It is found that larger surface roughness can increase the coercivity of the thin films [28]–[31], which is due to the formation of more pinning sites that pin domain walls. Because the Co layer is thin in our $[\text{Co}/\text{Pt}]_n$ multilayers, the domain wall may be a Néel wall [31]. The Néel wall is characterized by its domain wall energy and domain wall thickness. The surface roughness causes the fluctuations in the domain wall energy. When the domain wall width is smaller than the surface/interface inhomogeneity, the higher interface roughness enhances the domain wall pinning sites, hence the coercivity [30], which well explains the coercivity in our $[\text{Co}/\text{Pt}]_n$ multilayers when $t_{\text{Co}} > 1.0$ nm.

IV. CONCLUSION

In conclusion, top- and bottom-pinned perpendicular $[\text{Co}/\text{Pt}]_n$ multilayers have been systematically investigated. With varying thickness of the cobalt layer that is coupled with the IrMn layer, the exchange bias and coercivity shows interesting changes for both multilayers. By tailoring the magnetization reversal of $[\text{Co}/\text{Pt}]_n$ multilayers, one may achieve a superparamagnetic state, an out-of-plane single domain state, an out-of-plane multi-domain state, and an in-plane state. These results may be helpful in designing magnetic media and other devices with different switching fields.

ACKNOWLEDGMENT

This work was supported by Science Foundation Ireland as part of MANSE project, and by the Ireland-China Scientific Exchange Scheme. The authors are also grateful for the partial support of the State Key Project of Fundamental Research, Ministry of Science and Technology (MOST), under Grant 2006CB932200, Chinese National Natural Science Foundation (NSFC), under Grants 10574156, 50528101 and 50721001, and Ireland-China Joint Research Project between SFI and MOST.

REFERENCES

- [1] S. S. P. Parkin, K. P. Roche, M. G. Samant, P. M. Rice, R. B. Beyers, R. E. Scheuerlein, E. J. O'Sullivan, S. L. Brown, J. Buchigano, D. W. Abraham, Y. Lu, M. Rooks, P. L. Trouilloud, R. A. Wanner, and W. J. Gallagher, "Exchange-biased magnetic tunnel junctions and application to nonvolatile magnetic random access memory," *J. Appl. Phys.*, vol. 85, pp. 5828–5833, 1999.
- [2] P. P. Freitas, R. Ferreira, S. Cardoso, and F. Cardoso, "Magnetoresistive sensors," *J. Phys.: Condens. Matter*, vol. 19, p. 165221, 2007.
- [3] B. Dieny, V. S. Speriosu, S. S. P. Parkin, B. A. Gurney, D. R. Wilhoit, and D. Mauri, "Giant magnetoresistive in soft ferromagnetic multilayers," *Phys. Rev. B*, vol. 43, p. 1297, 1991.
- [4] S. Tehrani, J. M. Slaughter, M. Deherrera, B. N. Engel, N. D. Rizzo, J. Slater, M. Durlam, R. W. Dave, J. Janesky, B. Butcher, K. Smith, and G. Grynkeiwich, "Magnetoresistive random access memory using magnetic tunnel junctions," *Proc. IEEE*, vol. 91, no. 3, p. 703, Mar. 2003.
- [5] X. F. Han, Z. C. Wen, and H. X. Wei, "Nanoring magnetic tunnel junction and its application in magnetic random access memory demo devices with spin-polarized current switching," *J. Appl. Phys.*, vol. 103, p. 07E933, 2008.
- [6] S. Maat, K. Takano, S. S. P. Parkin, and E. E. Fullerton, "Perpendicular exchange bias of Co/Pt multilayers," *Phys. Rev. Lett.*, vol. 87, p. 087202, 2001.
- [7] O. Hellwig, S. Maat, J. B. Kortright, and E. E. Fullerton, "Magnetic reversal of perpendicularly-biased Co/Pt multilayers," *Phys. Rev. B*, vol. 65, p. 144418, 2002.
- [8] Z. Y. Liu and S. Adenwalla, "Closely linear temperature dependence of exchange bias and coercivity in out-of-plane exchange-biased $[\text{Pt}/\text{Co}]_3/\text{NiO}$ (11 Å) multilayer," *J. Appl. Phys.*, vol. 94, p. 1105, 2003.
- [9] J. Sort and B. Dieny, "Perpendicular exchange bias in antiferromagnetic-ferromagnetic nanostructures," *Appl. Phys. Lett.*, vol. 84, pp. 3696–3698, 2004.
- [10] G. Malinowski, M. Albrecht, I. L. Guhr, J. M. D. Coey, and S. van Dijken, "Size-dependent scaling of perpendicular exchange bias in magnetic nanostructures," *Phys. Rev. B*, vol. 75, p. 012413, 2007.
- [11] J. Sort, V. Baltz, F. Garcia, B. Rodmacq, and B. Dieny, "Tailoring perpendicular exchange bias in Pt/Co-IrMn multilayers," *Phys. Rev. B*, vol. 71, p. 054411, 2005.
- [12] F. Garcia, J. Sort, B. Rodmacq, S. Auffret, and B. Dieny, "Large anomalous enhancement of perpendicular exchange bias by introduction of a nonmagnetic spacer between the ferromagnetic and antiferromagnetic layers," *Appl. Phys. Lett.*, vol. 83, pp. 3537–3539, 2003.
- [13] S. van Dijken, J. Moritz, and J. M. D. Coey, "Correlation between perpendicular exchange bias and magnetic anisotropy in $\text{IrMn}/[\text{Co}/\text{Pt}]_n$ and $[\text{Pt}/\text{Co}]_n/\text{IrMn}$ multilayers," *J. Appl. Phys.*, vol. 97, p. 063907, 2005.
- [14] F. Garcia, J. Moritz, F. Ernult, S. Auffret, B. Rodmacq, B. Dieny, J. Camarero, Y. Pennec, S. Pizzini, and J. Vogel, *J. Exp. Mar. Biol. Ecol.*, vol. 38, p. 2730, 2002.
- [15] J. F. Feng, G. Feng, J. M. D. Coey, X. F. Han, and W. S. Zhan, "High inverted tunneling magnetoresistance in MgO-based magnetic tunneling junctions," *Appl. Phys. Lett.*, vol. 91, p. 102505, 2007.
- [16] P. Lemoine, J. P. Quinn, P. D. Maguire, and J. A. D. McLaughlin, "Measuring the thickness of ultra-thin diamond-like carbon films," *Carbon*, vol. 44, pp. 2617–2624, 2006.
- [17] G. M. B. Castro, J. Geshev, J. E. Schmidt, E. B. Saitovich, and L. C. C. M. Nagamine, "Cone magnetization state and exchange bias in $\text{IrMn}/\text{Cu}/[\text{Co}/\text{Pt}]_3$ multilayers," *J. Appl. Phys.*, vol. 106, p. 113922, 2009.
- [18] Y. L. Lunin, Y. P. Kabanov, V. I. Nikitenko, X. M. Cheng, D. Clarke, O. A. Tretiakov, O. Tchernyshyov, A. J. Shapiro, R. D. Shull, and C. L. Chien, "Asymmetric domain nucleation and unusual magnetization reversal in ultrathin Co films with perpendicular anisotropy," *Phys. Rev. Lett.*, vol. 98, p. 117204, 2007.
- [19] J. Nogués and I. K. Schuller, "Exchange bias," *J. Magn. Magn. Mater.*, vol. 192, p. 203, 1999.
- [20] M. K. Chan, J. S. Parker, P. A. Crowell, and C. Leighton, "Identification and separation of two distinct contributions to the training effect in polycrystalline Co/FeMn bilayers," *Phys. Rev. B*, vol. 77, p. 014420, 2008.
- [21] S. Brems, K. Temst, and C. V. Haesendonck, "Origin of the training effect and asymmetry of the magnetization in polycrystalline exchange bias systems," *Phys. Rev. Lett.*, vol. 99, p. 067201, 2007.
- [22] J. R. Rhee, "Exchange bias in $[\text{Pt}/\text{Co}]_n/\text{IrMn}$ multilayers with perpendicular magnetic anisotropy," *J. Appl. Phys.*, vol. 101, p. 09E523, 2007.
- [23] W. H. Meiklejohn and C. P. Bean, "New magnetic anisotropy," *Phys. Rev.*, vol. 102, p. 1413, 1956.
- [24] W. H. Meiklejohn, "Exchange anisotropy—A review," *J. Appl. Phys.*, vol. 33, p. 1328, 1962.
- [25] M. T. Johnson, P. J. H. Bloemen, F. J. A. den Broeder, and J. J. de Vries, "Magnetic anisotropy in metallic multilayers," *Rep. Prog. Phys.*, vol. 59, pp. 1409–1458, 1996.
- [26] C. Liu, C. Yu, H. Jiang, L. Shen, C. Alexander, and G. J. Mankey, "Effect of interface roughness on the exchange bias for NiFe/FeMn," *J. Appl. Phys.*, vol. 87, p. 6644, 2000.
- [27] D. L. Mobley, C. R. Pike, J. E. Davies, D. L. Cox, and R. R. P. Singh, "Hysteresis loops of Co-Pt perpendicular magnetic multilayers," *J. Phys.: Condens. Matter*, vol. 16, pp. 5897–5906, 2004.
- [28] C.-H. Chang and M. H. Kryder, "Effect of substrate roughness on microstructure, uniaxial anisotropy, and coercivity of Co/Pt multilayer thin films," *J. Appl. Phys.*, vol. 75, pp. 6864–6866, 1994.
- [29] Q. Jiang, H.-N. Yang, and G.-C. Wang, "Effect of surface roughness on hysteresis loops of ultrathin Co films from 2ML to 30ML on Cu (001) surface," *Surf. Sci.*, vol. 373, p. 181, 1997.
- [30] J. Swerts, K. Temst, N. Vandamme, C. Van Haesendonck, and Y. Bruynseraede, "Interplay between surface roughness and magnetic properties in Ag/Fe bilayers," *J. Magn. Magn. Mater.*, vol. 240, pp. 380–382, 2002.
- [31] A. Hubert and R. Schafer, *Magnetic Domains*. Berlin: Springer-Verlag, 1998.